Revue des Composites et des Matériaux Avancés-Journal of Composite and Advanced Materials
Vol. 36, No. 1, February, 2026, pp. 53-58
Journal homepage: http://iieta.org/journals/rcma

Influence of Floral Extract Phytochemistry on the Structural and Optical Properties of Green-Synthesized Iron Oxide Nanoparticles

Noorhan T. Muhammad, Bilal K. Al-Rawi*

Department of Physics, College of Education for Pure Science, University of Anbar, Al Rumadi 31001, Iraq

Corresponding Author Email: sc.bilal_alrawi@uoanbar.edu.iq

https://doi.org/10.18280/rcma.360105

Received: 17 July 2025
Revised: 18 September 2025
Accepted: 15 February 2026
Available online: 28 February 2026

Keywords:
green synthesis, iron oxide nanoparticles, phytochemistry, plant extracts, Rosa damascena, structural properties, optical properties

ABSTRACT

The phytochemical composition of plant extracts plays a decisive role in modulating the properties of nanoparticles synthesized via green routes. This study systematically investigates how aqueous extracts from three distinct floral sources—*Rosa damascena* (Damask rose), *Rosa chinensis* (Chinese rose), and *Moringa oleifera*—influence the formation, structure, and optical characteristics of iron oxide nanoparticles (FeOx NPs). Using ferric chloride as the iron precursor and sodium hydroxide for pH adjustment, NPs were synthesized under identical conditions to isolate the effect of the extract. Comprehensive characterization via X-ray diffraction (XRD), Field Emission Scanning Electron Microscopy (FESEM), Atomic Force Microscopy (AFM), and ultraviolet-visible (UV-Vis) spectroscopy revealed significant extract-dependent variations. XRD confirmed the crystalline Fe_3O_4/γ-Fe_2O_3 phase formation, with *R. damascena* extract yielding the sharpest peaks, indicating highest crystallinity, attributed to its rich polyphenolic content. FESEM and AFM showed quasi-spherical morphologies with varying degrees of agglomeration and surface roughness; *M. oleifera* produced larger particles (~100 nm) while *R. chinensis* yielded smaller ones (~27 nm). UV-Vis spectra exhibited characteristic ligand-to-metal charge transfer bands, with absorption intensity correlating with extract antioxidant capacity. The findings demonstrate that specific phytochemical profiles (e.g., flavonoids vs. proteins) directly govern nucleation kinetics, growth mechanisms, and final NP attributes. This work provides a fundamental understanding of plant-mediated synthesis and offers a guideline for tailoring FeOx NP properties for targeted applications in catalysis, biomedicine, or optics by selecting appropriate botanical precursors.

1. INTRODUCTION

Nanomaterials have become indispensable in modern scientific and technological domains due to the exceptional properties that distinguish them from their bulk counterparts. Defined by dimensions typically below 100 nanometers, these materials display enhanced surface-area-to-volume ratios, which directly contribute to superior chemical reactivity, improved catalytic behavior, size-dependent optical features, and the emergence of quantum confinement effects. These attributes have significantly advanced their use in various sectors, including environmental remediation, medical diagnostics, targeted drug delivery, sensors, and energy conversion and storage systems [1, 2].

Among the various classes of nanomaterials, iron oxide nanoparticles (Fe_2O_3 NPs) have attracted particular attention owing to their low toxicity, environmental stability, magnetic responsiveness, and biocompatibility. Their utility spans a broad spectrum of applications such as water purification, magnetic hyperthermia, lithium-ion batteries, and biosensing platforms. The ability to tailor their morphology, crystallinity, and surface chemistry at the nanoscale makes them highly versatile for integration into functional devices [3, 4].

In recent years, the focus has shifted toward green synthesis methods, which utilize biological entities such as plant extracts as reducing and capping agents to replace hazardous chemicals typically used in traditional physical or chemical nanoparticle production. This eco-friendly synthesis approach aligns with the 12 principles of green chemistry and offers a sustainable, low-cost alternative that minimizes environmental impact while ensuring nanoparticle stability and uniformity [5].

In this context, the present study employs floral extracts from Rosa damascena (Damask rose), Rosa chinensis (China rose), and Moringa oleifera as bio-reductants and stabilizers for the synthesis of Fe_2O_3 nanoparticles. These botanical sources are known to contain diverse phytochemicals, including flavonoids, polyphenols, terpenoids, and alkaloids that facilitate the reduction of ferric ions (Fe^{3+}) and control the growth of nanoparticles in aqueous solution. The selection of these specific plants was motivated by their high content of bioactive compounds, long-standing use in traditional medicine, broad ecological availability, and proven biocompatibility. Moreover, their comparative analysis under identical synthesis conditions enables the evaluation of how

variations in phytochemical composition affect the nucleation and stabilization of nanoparticles [6, 7].

The underlying mechanisms by which plant-derived phytochemicals facilitate nanoparticle formation primarily involve redox and capping processes. Compounds such as polyphenols, flavonoids, terpenoids, and saponins can donate electrons to ferric ions, reducing them to Fe_2O_3 nuclei while undergoing oxidation themselves. For example, phenolic hydroxyl groups may oxidize to quinones as they reduce Fe^{+3} to Fe^{+2} or Fe_3O_4. Simultaneously, these phytochemicals adsorb onto the nanoparticle surfaces, forming a protective organic layer that inhibits agglomeration and allows for better control over particle size and shape. This dual functionality reduction and stabilization is fundamental to the green synthesis strategy and underscores its value as a safer, scalable, and environmentally conscious alternative to conventional methods [8, 9].

While various biological systems, such as algae and fungi, have been employed in green nanoparticle synthesis due to their enzymatic or polysaccharide-based reducing capabilities, these methods often require sterile cultivation conditions, longer synthesis durations, and more complex handling. In contrast, floral extracts provide a simpler, more accessible alternative that leverages naturally abundant phytochemicals for rapid and effective nanoparticle formation [10, 11]. This study thus highlights the comparative advantage of flower-based synthesis in terms of operational ease, sustainability, and phytochemical diversity.

By exploring these natural extracts for nanoparticle synthesis, this work contributes not only to the advancement of green nanotechnology but also offers insights into the design of scalable, biocompatible methods that leverage abundant plant-based resources. The novelty of this study lies in its comparative evaluation of three distinct floral systems and their effectiveness in modulating nanoparticle characteristics under standardized parameters.

2. MATERIALS AND METHODS

2.1 Preparation of aqueous plant extracts

Aqueous extracts were prepared from three types of dried and ground plant materials:

Rosa damascena (Damask rose),

Rosa chinensis (Chinese rose), and

Moringa oleifera (Moringa rose).

For each extract, 1 gram of the dried plant material was mixed with 100 mL of distilled water in a glass beaker. The mixture was heated to 80°C on a magnetic stirrer with continuous stirring for 1 hour. After heating, the mixture was allowed to cool and left to stand at room temperature overnight. The following day, the solution was filtered using Whatman No. 1 filter paper to remove solid residues, and the resulting filtrate was collected as the aqueous plant extract. The process was initiated with the Rosa damascena extract and repeated for the other two plant types.

The ratio of 1 g plant material per 100 mL water was chosen based on preliminary optimization trials and literature evidence suggesting that this concentration provides sufficient phytochemical content for nanoparticle reduction and stabilization, while maintaining extract clarity and ease of handling.

Figure 1. A flowchart depicting the main steps of the plant-mediated synthesis of iron oxide nanoparticles

2.2 Green synthesis of iron oxide nanoparticles

Five grams of ferric chloride ($FeCl_3$) were dissolved in 100 mL of distilled water under constant magnetic stirring until fully dissolved. Then, 50 mL of the prepared Rosa damascena extract was added dropwise using a burette at 30°C under continuous stirring. After complete addition, the mixture was heated to 80°C. The pH of the solution was adjusted to ≥ 9 by adding 1 gram of sodium hydroxide (NaOH) dissolved in 100 mL of distilled water. This resulted in the formation of a dark brown precipitate, indicating the formation of iron oxide nanoparticles.

The reaction mixture was then left at room temperature overnight. On the following day, the precipitate was separated by filtration, washed with distilled water, and dried in a hot air oven at 80°C for 30 minutes. The dried product was subsequently calcined in a muffle furnace at 300–400°C for 2 hours to obtain iron oxide nanoparticles in powder form.

This temperature range was selected to ensure sufficient thermal decomposition of organic residues and promote crystallization. Lower temperatures (< 300°C) may result in incomplete phase formation, while higher temperatures (> 400°C) can cause undesirable grain growth or loss of surface-bound phytochemicals, thereby affecting particle stability.

The same synthesis procedure, including all concentrations and conditions, was applied using Rosa chinensis and Moringa oleifera extracts to prepare the other two nanoparticle samples.

2.3 Characterization techniques

The synthesized iron oxide nanoparticles were characterized using various analytical techniques. X-ray diffraction (XRD) revealed crystalline structure, Field

Emission Scanning Electron Microscopy (FESEM) provided morphological details, Atomic Force Microscopy (AFM) determined surface roughness, and UV–Vis spectroscopy estimated the band gap of the nanoparticles. Figure 1 shows the synthesis process.

Figure 1. Schematic illustration of the two-step green synthesis process: (1) preparation of aqueous plant extracts from Rosa damascena, Rosa chinensis, and Moringa oleifera; (2) formation of iron oxide nanoparticles via co-precipitation with $FeCl_3$/NaOH, followed by washing, drying, and calcination.

3. RESULT AND DISCUSSION

3.1 X-ray diffraction analysis

Figure 2 shows the XRD analysis of the crystalline structure of the iron oxide nanoparticles synthesized using green methods. The diffraction patterns for all three samples showed characteristic peaks indicating a crystalline structure with varying degrees of crystallinity. The major diffraction peaks were observed at 2θ values of approximately 30°, 33.35°, 35.5°, 43°, 53.5°, 57°, and 62.6°, corresponding to the 220, 311, 311, 400, 422, 511, and 440 crystal planes, respectively. These peaks are consistent with the standard diffraction patterns of magnetite (Fe_3O_4) and maghemite (γ-Fe_2O_3) phases, indicating successful formation of iron oxide nanoparticles through thermal decomposition of ferric chloride at 300–400℃ [12].

Although all samples exhibited similar peak positions, indicating the formation of comparable iron oxide phases, variations in peak intensity and width were observed. These differences reflect variations in crystallite size, purity, and degree of structural order among the samples, which are directly influenced by the type and composition of the plant extract used during synthesis.

Sample 1, prepared using Rosa damascena extract, showed the sharpest and most intense peaks, suggesting a higher degree of crystallinity and purity. This can be attributed to the high concentration of bioactive compounds such as phenolic acids, flavonoids, and anthocyanins, which are known to act as strong reducing and stabilizing agents during nanoparticle synthesis [13]. These compounds promote controlled nucleation and growth of iron oxide nanoparticles, resulting in well-ordered crystalline structures [14].

Sample 2, synthesized using Moringa oleifera extract, displayed slightly broader and less intense peaks, indicating lower crystallinity compared to Sample 1. Moringa is rich in proteins, amino acids, and polysaccharides, which also possess reducing capabilities, but may lead to less uniform nucleation and stabilization compared to polyphenol-rich extracts [15].

Sample 3, derived from Rosa chinensis extract, showed the weakest and broadest peaks, pointing to reduced crystallinity and less ordered structures. This may be due to the lower antioxidant content and higher fiber composition in the plant matrix, which limit the efficiency of reduction and stabilization processes during nanoparticle formation [16].

In addition to the qualitative observations, a comparative analysis of the full width at half maximum (FWHM) values of the most intense diffraction peaks was conducted to quantitatively assess the crystallinity of the synthesized nanoparticles. Sample 1 (Rosa damascena) exhibited the narrowest FWHM values, confirming the presence of well-crystallized particles with minimal lattice strain. In contrast, Samples 2 and 3 showed broader peaks, indicative of smaller crystallite sizes and higher defect densities. This trend supports the earlier qualitative interpretation, suggesting that the phytochemical composition of each extract significantly influences the nucleation rate, growth kinetics, and final crystal quality of the iron oxide nanoparticles.

The observed differences in crystallinity and peak sharpness among the three samples may be directly attributed to the nature and concentration of plant-specific phytochemicals involved in the synthesis process. For instance, Rosa damascena contains a high abundance of phenolic compounds and flavonoids, which not only facilitate efficient reduction of Fe^{3+} ions but also promote uniform nucleation and limit structural defects, leading to higher phase purity. In contrast, the relatively broader peaks in Moringa oleifera and Rosa chinensis samples suggest less ordered crystalline phases, potentially due to less effective capping or slower reduction kinetics caused by proteins or fibrous components.

These findings reinforce the idea that phytochemical diversity and concentration in plant extracts play a crucial role not only in initiating nanoparticle formation but also in determining the structural integrity and phase quality of the final product.

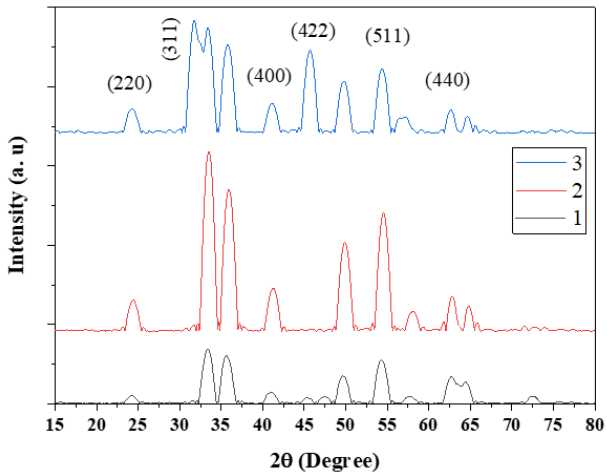

Figure 2. The X-ray diffraction (XRD) of the prepared compounds

3.2 Field Emission Scanning Electron Microscopy analysis

Figure 3 presents the FESEM images of iron oxide nanoparticles synthesized using Rosa damascena, Moringa oleifera, and Rosa chinensis extracts. The images reveal that the particles generally exhibit a quasi-spherical morphology with varying degrees of surface roughness and aggregation. Notably, significant agglomeration is observed in all three samples, which is commonly attributed to the intrinsic magnetic interactions and high surface energy of iron oxide nanoparticles.

Sample 1 (Rosa damascena) displayed the formation of unique nanotube-like structures with diameters reaching approximately 70.3 nm. This suggests a directional growth behavior potentially induced by specific phytochemicals such as flavonoids and anthocyanins present in the extract. Sample 2 (Moringa oleifera) exhibited a dense assembly of larger spherical particles with average sizes around 100.1 nm, whereas Sample 3 (Rosa chinensis) showed smaller, more irregular particles averaging 26.8 nm in diameter.

The differences in particle size and morphology across the samples can be directly correlated with the composition of the plant extracts used in the green synthesis. Polyphenol-rich extracts (e.g., Rosa damascena) appear to support more controlled nucleation and growth, while protein- or fiber-dominant extracts (e.g., Moringa and Rosa chinensis) may lead to less uniform stabilization.

Although the green synthesis route effectively produced nanoscale structures, the presence of pronounced agglomeration remains a notable limitation. No surfactants or dispersion techniques were applied in the current synthesis, which may have allowed for secondary clustering. To address this in future work, the incorporation of biocompatible surfactants (such as PVP or CTAB) or the application of ultrasonication could be considered to improve dispersion and reduce aggregation while maintaining green chemistry principles.

3.3 Atomic Force Microscopy analysis

Figure 4 shows the AFM of the samples, revealing fine details of the distribution and height of nanoparticles on the sample surface.

AFM images showed that the samples synthesized via green methods exhibited significant variation in particle size and distribution, along with a relatively rough and irregular surface. This variation is attributed to the interaction of natural organic compounds present in the plant extracts used during the synthesis process, which directly influences the final surface morphology of the nanoparticles [17-19].

3.4 Ultraviolet–Visible spectroscopy analysis

Ultraviolet–Visible (UV–Vis) spectroscopy was employed to investigate the optical properties of the synthesized iron oxide nanoparticles. The measurements were conducted in the spectral range of 200–800 nm to identify the characteristic absorption behavior of the samples prepared using different plant extracts (Figure 5).

All three samples exhibited distinct absorption bands within the 200–500 nm range. Prominent peaks were observed at approximately 270–280 nm and 360–370 nm, along with a weaker absorption band around 420 nm. These bands are primarily attributed to Ligand-to-Metal Charge Transfer (LMCT) transitions from oxygen ligands to Fe^{3+} ions, as well as d–d electronic transitions within the iron ions themselves [20]. Similar absorption features have been consistently reported in the literature for iron oxide nanoparticles synthesized via green methods [21].

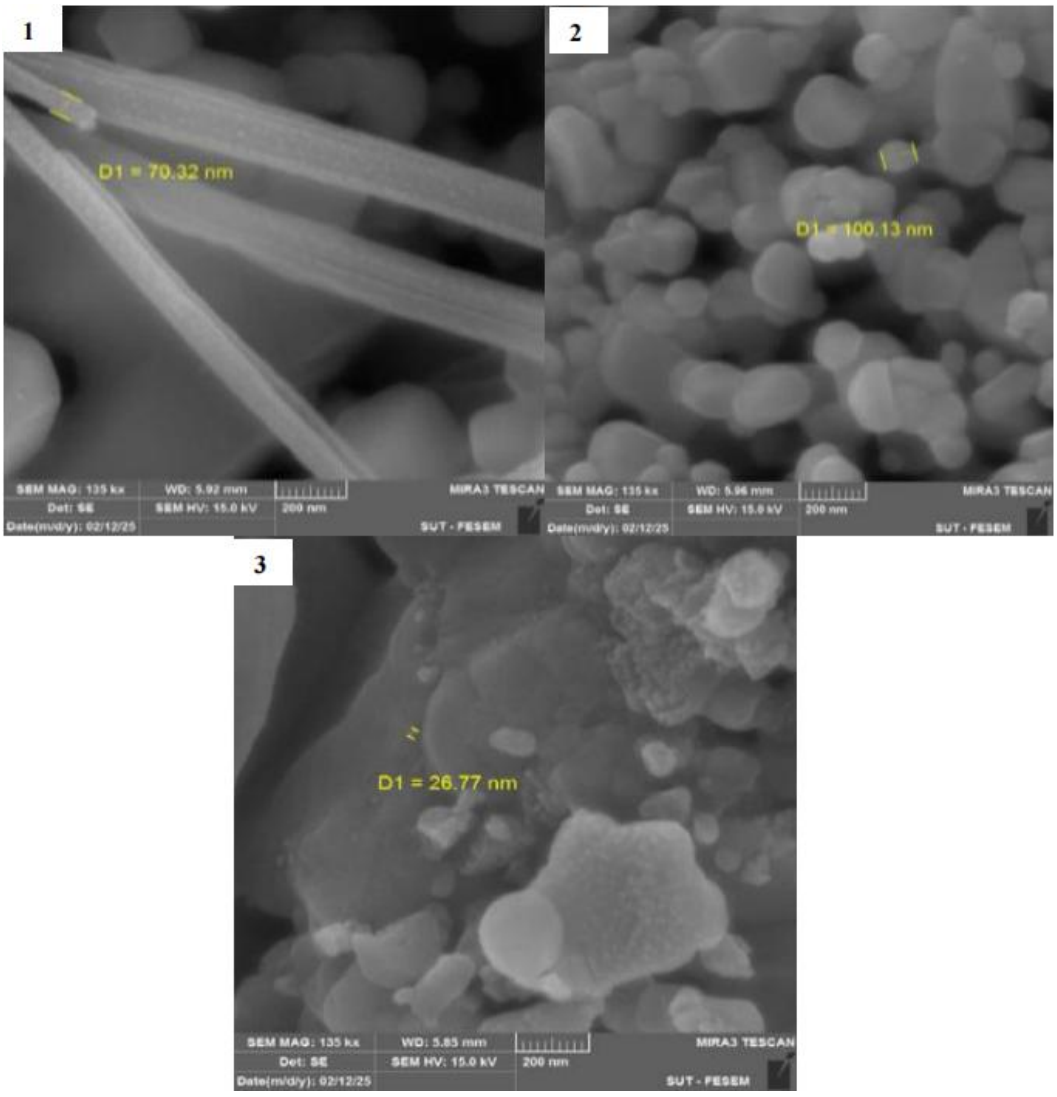

Figure 3. Field Emission Scanning Electron Microscopy (FESEM) of the prepared compounds

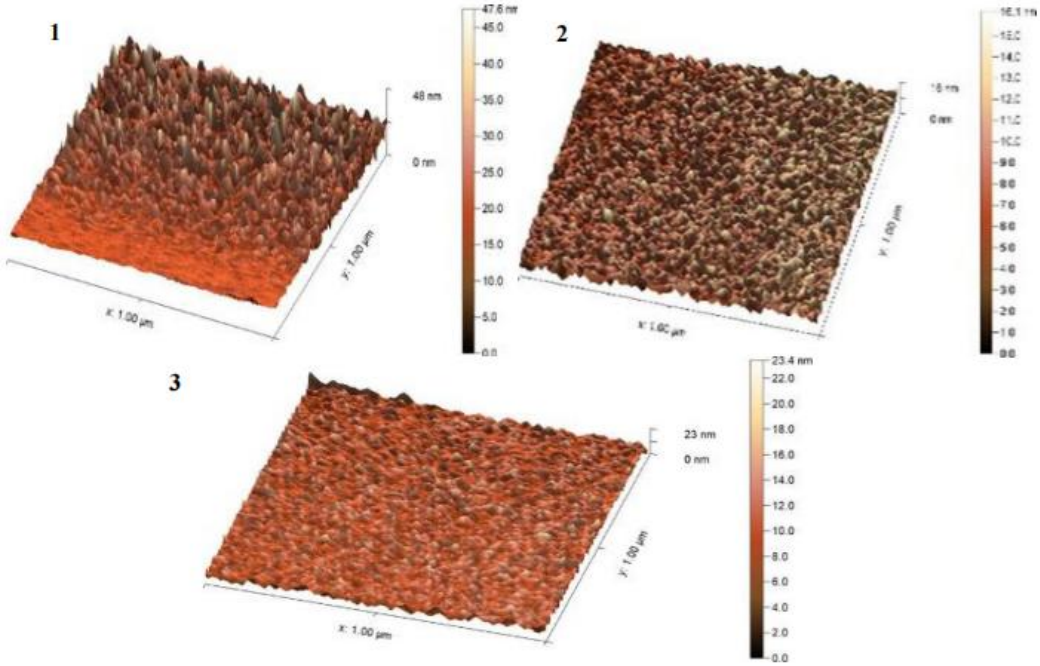

Figure 4. Atomic Force Microscopy (AFM) of the prepared compounds

Notably, Sample 3, synthesized using Rosa chinensis (Chinese rose) extract, demonstrated the highest absorbance intensity across the measured range. This suggests enhanced stabilization of the nanoparticles, likely due to the presence of phenolic compounds and flavonoids in the extract. These biomolecules serve not only as reducing agents but also as effective capping agents, preventing nanoparticle agglomeration and promoting the formation of smaller, more monodisperse particles with higher optical activity [22].

These findings underscore the significant role of the phytochemical composition of the plant extract in modulating the optical and structural characteristics of the resulting nanoparticles.

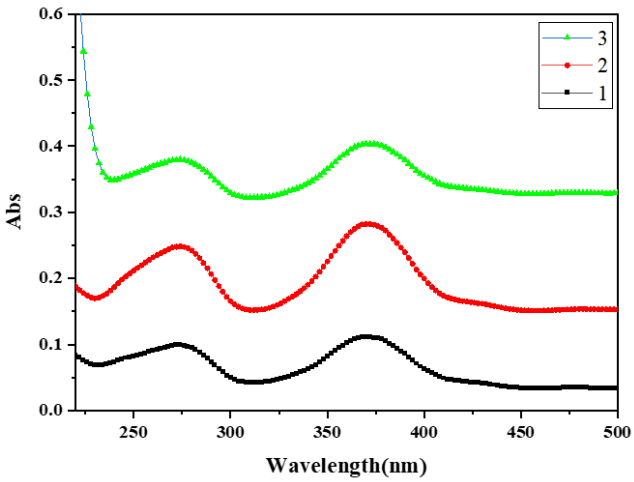

Figure 5. Ultraviolet–Visible (UV–Vis) of the prepared compounds

4. CONCLUSIONS

This study confirms the effectiveness of the green synthesis method in preparing iron oxide nanoparticles using aqueous plant extracts from Rosa damascena, Moringa oleifera, and Rosa chinensis. Rich in phenolic compounds, flavonoids, and antioxidants, these extracts acted as natural reducing and stabilizing agents, offering an environmentally friendly alternative to conventional chemical methods.

XRD results revealed the successful formation of iron oxide nanoparticles with crystalline structures, where differences in peak intensity reflected the influence of extract composition on crystallinity. Field-Emission Scanning Electron Microscopy (FESEM) showed quasi-spherical particles with observable agglomeration, highlighting the role of plant-derived compounds in morphology control. UV–Vis spectroscopy confirmed characteristic LMCT transitions, with variations in absorption intensity supporting differences in phytochemical content.

Although the synthesized nanoparticles showed promising structural and optical properties, particularly when using Rosa damascena extract, their potential applications, such as in catalysis, water treatment, or biomedicine, remain speculative at this stage. Further investigations, including in vitro cytotoxicity tests and functional performance evaluations, are essential to validate their practical applicability in biomedical or environmental fields.

REFERENCES

[1] Norhasri, M.M., Hamidah, M.S., Fadzil, A.M. (2017). Applications of using nano material in concrete: A review. Construction and Building Materials, 133: 91-97. https://doi.org/10.1016/j.conbuildmat.2016.12.005

[2] Thabit, W.S., Al-Rawi, B.K. (2023). The effect of atomization force on the structural properties of NiTi thin films. International Journal of Nanoscience, 22(2): 2350005. https://doi.org/10.1142/S0219581X23500059

[3] Pourmadadi, M., Rahmani, E., Shamsabadipour, A., Mahtabian, S., Ahmadi, M., Rahdar, A., Díez-Pascual, A.M. (2022). Role of iron oxide (Fe_2O_3) nanocomposites in advanced biomedical applications: A state-of-the-art

review. Nanomaterials, 12(21): 3873. https://doi.org/10.3390/nano12213873

[4] Kumar, Y., Sinha, A.S.K., Nigam, K.D.P., Dwivedi, D., Sangwai, J.S. (2023). Functionalized nanoparticles: Tailoring properties through surface energetics and coordination chemistry for advanced biomedical applications. Nanoscale, 15(13): 6075-6104. https://doi.org/10.1039/D2NR07163K

[5] Khathim, S.A.E., Al-Rawi, B.K., Khalaf, M.K. (2024). Surface modification of NiTi alloy with sputtered tantalum coatings to improve its hardness, corrosion resistance and biocompatibility. International Journal of Nanoscience, 23(3): 2350073. https://doi.org/10.1142/S0219581X23500734

[6] Arif, M.R., Hussain, A., Najam, A., Sattar, A., Yaqub, S., Asif, A., Gorsi, F.I., Ahmed, A., Firdous, N., Elkhedir, A.E., Wang, Y. (2025). Traditional uses, phytochemistry, and pharmacology of *Flemingia macrophylla*, an important traditional medicinal plant. Discover Pharmaceutical Sciences, 1(1): 2. https://doi.org/10.1007/s44395-025-00003-7

[7] Singh, A., Bharti, R., Thakur, A., Verma, M., Sharma, R. (2024). Leaf extract mediated green synthesis of iron-oxide nanoparticles (FeO-NPs) by using *Hibiscus rosa-sinensis* (China rose): A potential approach and its biological application. Orbital: The Electronic Journal of Chemistry, 16(4): 271-278. https://doi.org/10.17807/orbital.v16i4.21174

[8] Fu, L. (2023). Pathways to Green Nanomaterials: Plants as Raw Materials, Reducing Agents and Hosts. Bentham Science Publishers.

[9] Dubey, R.K., Shukla, S., Hussain, Z. (2023). Green synthesis of silver nanoparticles; A sustainable approach with diverse applications. Chinese Journal of Applied Physiology, 39: e20230007. https://doi.org/10.62958/j.cjap.2023.007

[10] Ślusarczyk, J., Adamska, E., Czerwik-Marcinkowska, J. (2021). Fungi and algae as sources of medicinal and other biologically active compounds: A review. Nutrients, 13(9): 3178. https://doi.org/10.3390/nu13093178

[11] Jamatia, T., Das, M.K., Mazumder, R. (2025). Floral extracts promising avenue for sustainable approach for nanoparticles: An updated review. Nanotechnology for Environmental Engineering, 10(2): 1-29. https://doi.org/10.1007/s41204-025-00423-x

[12] Al-Rashid, S.N.T. (2024). Study of the variations of quantum confinement energy with the exciton Bohr radius of zinc selenide. Nanoscience and Technology: An International Journal, 15(3): 21-27. https://doi.org/10.1615/NanoSciTechnolIntJ.2023048643

[13] Mohammed, S.A.J., Al-Haddad, R.M., Al-Rawi, B.K. (2024). Structural and optical properties of magnetite nanoparticles prepared by green method for biophysics applications. Nanoscience and Technology: An International Journal, 15(2): 95-105. https://doi.org/10.1615/NanoSciTechnolIntJ.2023048382

[14] Mazhir, S.N., Ali, A.H., Abdalameer, N.K., Qasim, S.A. (2022). ZnO: Fe_3O_4 nanoparticles produced by cold plasma: Synthesis, characterization and anti-microbial activity. International Journal of Nanoscience, 21(3): 2250021. https://doi.org/10.1142/S0219581X22500211

[15] Hussain, A.M., Al-Rawi, B.K. (2024). Synthesis and characterizations of physical and antibacterial properties of the Ag nanoparticles by exploding of wire technique. International Journal of Nanoscience, 23(3): 2350075. https://doi.org/10.1142/S0219581X23500758

[16] Kiwumulo, H.F., Muwonge, H., Ibingira, C., Lubwama, M., Kirabira, J.B., Ssekitoleko, R.T. (2022). Green synthesis and characterization of iron-oxide nanoparticles using Moringa oleifera: A potential protocol for use in low and middle income countries. BMC Research Notes, 15(1): 149. https://doi.org/10.1186/s13104-022-06039-7

[17] Al-Rawi, B.K., Aljanabi, S.M. (2021). Modeling the physical properties of ZnO nanoparticles with selective hydrogen using DFT. International Journal of Nanoscience, 20(1): 2150011. https://doi.org/10.1142/S0219581X21500113

[18] Jamshidiyan, M., Shirani, A.S., Alahyarizadeh, G.H. (2017). Solvothermal synthesis and characterization of magnetic Fe_3O_4 nanoparticle by different sodium salt sources. Materials Science-Poland, 35(1): 50-57. https://doi.org/10.1515/msp-2017-0004

[19] Iravani, S. (2011). Green synthesis of metal nanoparticles using plants. Green Chemistry, 13(10): 2638-2650. https://doi.org/10.1039/C1GC15386B

[20] Bilton, M., Milne, S., Brown, A. (2012). Comparison of hydrothermal and sol-gel synthesis of nano-particulate hydroxyapatite by characterisation at the bulk and particle level. Open Journal of Inorganic Non-Metallic Materials, 2(1): 1-10. https://doi.org/10.4236/ojinm.2012.21001

[21] Suppiah, D.D., Julkapli, N.M., Sagadevan, S., Johan, M.R. (2023). Eco-friendly green synthesis approach and evaluation of environmental and biological applications of iron oxide nanoparticles. Inorganic Chemistry Communications, 152: 110700. https://doi.org/10.1016/j.inoche.2023.110700

[22] Younis, I.Y., El-Hawary, S.S., Eldahshan, O.A., Abdel-Aziz, M.M., Ali, Z.Y. (2021). Green synthesis of magnesium nanoparticles mediated from Rosa floribunda charisma extract and its antioxidant, antiaging and antibiofilm activities. Scientific Reports, 11(1): 16868. https://doi.org/10.1038/s41598-021-96377-6